PROCEEDINGS OF SPIE

SPIEDigitalLibrary.org/conference-proceedings-of-spie

3D printed micro-scale fiber optic probe for intravascular pressure sensing

Radhika K. Poduval, Jo Coote, Charles A. Mosse, Malcolm C. Finlay, Ioannis Papakonstantinou, et al.

Radhika K. Poduval, Jo Coote, Charles A. Mosse, Malcolm C. Finlay, Ioannis Papakonstantinou, Adrien E. Desjardins, "3D printed micro-scale fiber optic probe for intravascular pressure sensing," Proc. SPIE 10728, Biosensing and Nanomedicine XI, 107280B (5 September 2018); doi: 10.1117/12.2321980

SPIE.

Event: SPIE Nanoscience + Engineering, 2018, San Diego, California, United States

3-D printed micro-scale fiber-optic probe for intravascular pressure sensing

Radhika K. Poduval[a], Joanna Coote[b,c], Charles A. Mosse[b,c], Malcolm C. Finlay[b,c,d], Ioannis Papakonstantinou[a,*], Adrien E. Desjardins[b,c]

[a]Department of Electronic and Electrical Engineering, University College London, UK
[b]Department of Medical Physics and Biomedical Engineering, University College London, UK
[c]Wellcome/EPSRC Centre for Interventional and Surgical Sciences, University College London, UK
[d]William Harvey Cardiovascular Research Institute, Queen Mary University of London, UK

ABSTRACT

Small form-factor invasive pressure sensors are widely used in minimally invasive surgery, for example to guide decision making in coronary stenting procedures. Current fiber-optic sensors can have high manufacturing complexities and costs, which severely constrains their adoption outside of niche fields. A particular challenge is the ability to rapidly prototype and iterate upon sensor designs to optimize performance for different applications and medical devices. Here, we present a new sensor fabrication method, which involves two-photon polymerization printing and integration of the printed structure onto the end-face of a single-mode optical fiber. The active elements of the sensor were a pressure-sensitive diaphragm and an intermediate temperature-sensitive spacer that was insensitive to changes in external pressure. Deflection of the diaphragm and thermal expansion the spacer relative to the fiber end-face were monitored using phase-resolved low-coherence interferometry. Pressure changes of 0.38 mmHg were detectable in the range of 760 to 1060 mmHg (absolute pressure), while a temperature changes of 0.023 °C were detectable in the range 25 to 47 °C using this fiber optic sensor. This method will enable the fabrication of a wide range of fiber-optic sensors with pressure and temperature sensitivities suitable for guiding minimally invasive surgery.

Keywords: Two-photon polymerization, fiber-optic sensor, minimally invasive surgery, low coherence interferometry

1. INTRODUCTION

Fiber-optic sensors can be invaluable for guiding diagnosis and therapy in minimally invasive surgery. For instance, invasive blood pressure and temperature measurements performed across a coronary artery stenosis are used to assess whether stent placement is needed[1]. Fiber-optic sensors can have several properties that are favorable for medical applications, including immunity to electromagnetic interference, MRI compatibility, and high mechanical flexibility. Moreover, their diminutive lateral dimensions are well suited to integration within existing devices and needles[2,3].

Several types of fiber-optic pressure sensors for medical applications have been developed, as reviewed by Poeggel *et al*.[4] and Roriz *et al*.[4,5]. These sensors frequently comprise a sealed gas cavity with a diaphragm. Deflections of the diaphragm that result from changes in external pressure can be monitored interferometrically with interrogation light delivered and received by the optical fiber. Interferometric detection can take place with a Fabry-Pérot cavity, provided that optical interfaces within the sensor have sufficiently high reflectivities[6]. Alternatively, detection can take place with low-coherence interferometry (LCI) if interfaces have relatively low optical reflectivities, such as the interfaces between a gas and inorganic or organic materials.

*i.papakonstantinou@ucl.ac.uk

Biosensing and Nanomedicine XI, edited by Hooman Mohseni, Massoud H. Agahi, Manijeh Razeghi, Proc. of SPIE Vol. 10728, 107280B · © 2018 SPIE
CCC code: 0277-786X/18/$18 · doi: 10.1117/12.2321980

As fiber-optic pressure and temperature sensors for minimally invasive surgery typically must have sub-millimeter lateral dimensions (for instance, to be integrated within a coronary guidewire), diaphragms often have micron-scale thicknesses to ensure detectable deflection in the presence of physiological pressure changes. This constraint necessitates precise micromachining methods. One method involves anodic bonding of a thin silicon diaphragm onto a glass support structure, but it tends to be very expensive in terms of the assembly time and capital equipment required[7]. To date, a microfabrication method that allows for rapid prototyping of different pressure sensing designs has been elusive.

Here, we investigate how two-photon polymerization (TPP) printing[8] can be applied to fabricate fiber-optic pressure and temperature sensors. It is based on the simultaneous absorption of two photons, which allows for downstream crosslinking of a resist material at a confined elliptical focal spot, whilst leaving upstream material unchanged[9]. TPP is typically realized using a femtosecond laser beam with a tight focus that is scanned across the material. Subsequently, washout of unprocessed material is performed to generate the TPP-printed structure. The TPP process was first predicted theoretically in 1931 by Maria Göppert-Mayer[10], and first demonstrated experimentally soon after the invention of ruby laser in 1961.

Recently there has been significant interest in TPP microfabrication of structures directly onto the cleaved end-faces of optical fibers[11–15]. These structures have included bulk lensed structures[14,16], spiral structures[17], and spring elements[15]. In the study by Gissibl *et al.*[14], a microscale multi-lens assembly on optical fiber end-face with focusing for optical miniature instruments such as endoscopes was demonstrated; however, the air gaps between adjacent lens elements were not sealed, so that physiological pressure sensing would be infeasible. A challenge with applying TPP printing to the fabrication of pressure sensors is the creation of sealed gas cavities: washout of unmodified resist material typically requires a channel through which gas can subsequently pass.

Here we report a method to fabricate a fiber-optic pressure sensor that comprises a TPP-printed extrinsic sensor element with a gas sealed cavity and a diaphragm. The gas seal is created by integrating the extrinsic sensor element with an optical fiber. The diaphragm is created with TPP printing along with the extrinsic sensor element. A temperature-sensitive spacer element is also TPP-printed as part of the extrinsic sensor element. The integrated sensor was interrogated with LCI and characterized with a benchtop setup that allowed for physiological pressure variations.

2. METHODS AND MATERIALS

2.1 Extrinsic sensor element design

The extrinsic element of the fiber-optic pressure sensor comprised a single-material, cylindrical structure with multiple optically-reflecting surfaces along its axis (Figure 1). The pressure sensitive component was a thin polymer diaphragm (thickness: 3 μm; diameter: 200 μm) at the distal end of the cap. The temperature sensitive component was a polymer block segment (spacer of thickness: 60 μm) adjacent to the cleaved surface of the optical fiber. The diaphragm deflected with changes in external pressure, thereby changing the optical path length of back-reflected light. While the diaphragm element was sensitive to changes in both pressure and temperature, the intermediate polymer spacer was only sensitive to changes in temperature. To assist with manipulating the sensor element following fabrication, and to simplify the integration process, an additional lateral holding element was added to the design. The complete sensor element, including the lateral holding element, was designed using computer aided design (CAD) software (Autodesk Inventor, Autodesk Inc., San Rafael, CA, USA).

2.2 Two-photon polymerization

The extrinsic sensor element was fabricated on a glass substrate coated with Indium Tin Oxide (ITO), using a commercial TPP system (Photonic Professional, *Nanoscribe GmbH*) and its 25x objective. During TPP printing, polymerization inside a droplet of liquid UV curable resin (IP-S, *Nanoscribe GmbH*) was induced at the focus of a 780 nm femtosecond laser beam by two-photon absorption. The beam could be rapidly steered laterally (X-Y) within a block (229 × 229 μm) and built to a height of ~200 μm in the Z-axis. For fabricating structures larger than the predefined microscale volume, printing was performed across multiple blocks using relatively slow translation with an X-Y piezo stage; the complete structure was realized by stitching together the individual blocks.

The original 3D CAD design was converted from Standard Tessellation Language (STL) format to the native General Writing Language (GWL) data format of the TPP system using DeScribe software (*Nanoscribe GmbH*). One of the tasks of this software was to partition the design into blocks; care was taken to ensure that the pressure-sensitive diaphragm was fully within in one block to avoid stitching errors. Subsequently, the GWL file was loaded into the system's control software NanoWrite (*Nanoscribe GmbH*) for print execution. After TPP printing, development in propylene-glycol monomethyl-ether-acetate (PGMEA) solvent for 180 minutes was performed to ensure complete washout of uncured resist from the complete structure, and subsequent rinsing in isopropyl-alcohol (IPA) for 15 minutes was performed to ensure removal of residual developer. The 3D printed structures were lifted-off the ITO-glass substrate with extra-fine tip, acid-resistant tweezers. These steps are represented schematically in Figure 2 (a)-(c).

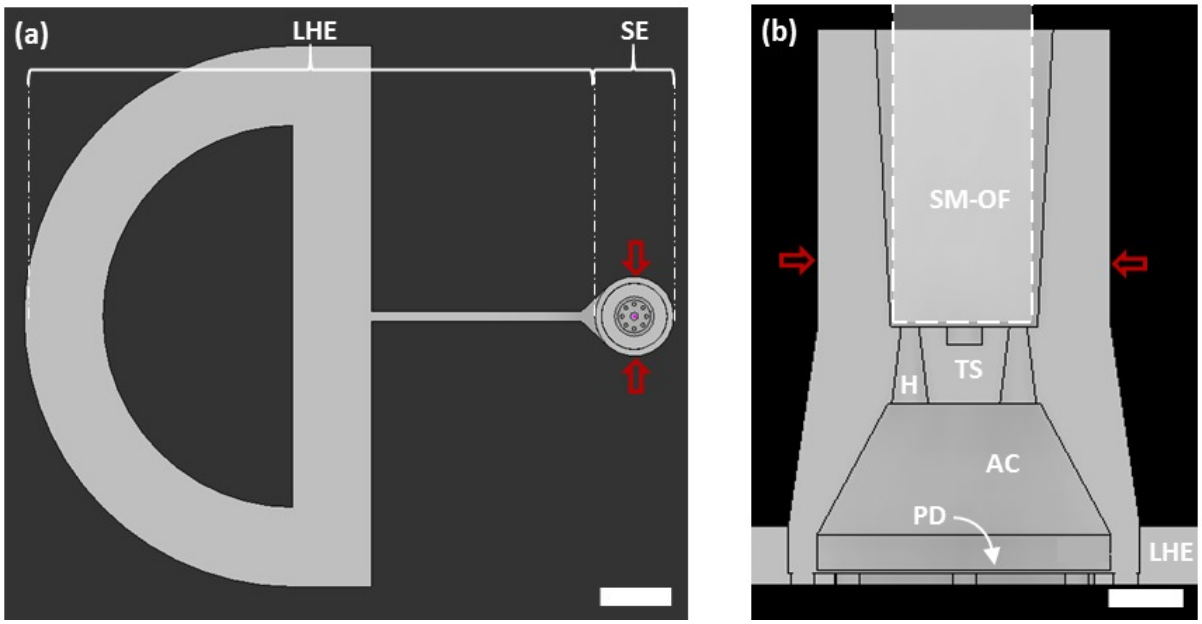

Figure 1. Computer aided design (CAD) designs. **(a)** Top view of the of the complete printed structure, which included the extrinsic sensor element (SE) and the much larger lateral holding element (LHE) that facilitated manipulation during fiber-optic integration. Scale bar: 200 µm. **(b)** Cross-sectional view of the SE (between arrows), showing the pressure-sensitive diaphragm (PD), the temperature-sensitive spacer (TS), the air cavity area between PD and TS (AC), and conical holes (H) within the TS. White dotted lines indicate the location where a single-mode optical fiber (SM-OF) was integrated. Scale bar: 50 µm.

2.3 Sensor integration

The TPP-printed extrinsic sensor element was integrated with a single-mode optical fiber (SM800, Thorlabs, NJ, USA) under an optical microscope (Figure 2(d)). It was held by the lateral holding element with tweezers, and temporarily affixed to a vertical optical post connected to a 3-axis manual translation stage facing the distal end of the optical fiber cleaved at normal incidence. The relative position of the extrinsic sensor element and the optical fiber was controlled by manual manipulation of the translation stage. The position of the distal end of the optical fiber within the extrinsic sensor element was monitored with low-coherence interferometry (Section 2.4). A small amount of UV-curable adhesive (Norland Optical Adhesive no. 81, Norland Products, NJ, USA) was applied to the proximal end of the fiber-affixed printed sensor element, and exposed to UV light from a light emitting diode (nominal central wavelength: 365 nm; M365FP1, Thorlabs, NJ, USA) for 5 minutes to ensure complete curing. After fiber-optic integration, the lateral holding element was readily snapped off with tweezers.

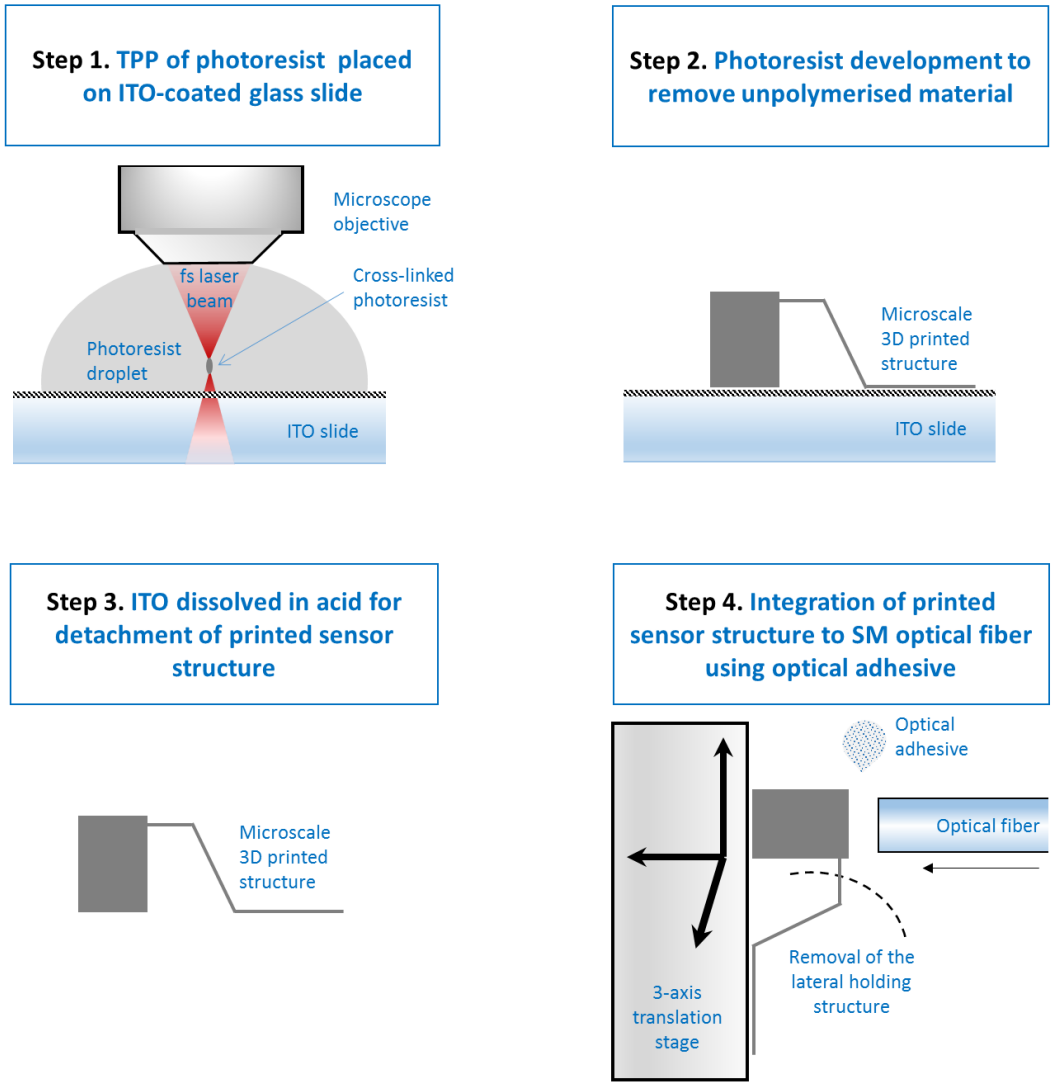

Figure 2. Schematic of the steps involved with microfabrication of the TPP-printed extrinsic sensor element (steps 1-3), and optical fiber integration (step 4). TPP: two-photon polymerization, ITO: Indium Tin Oxide, SM: single-mode.

2.4 Low coherence interferometry

Light from the optical fiber was guided to the extrinsic sensing element, where each interface formed a reflective surface due to the refractive index difference (Figure 3). Light passing through each interface was partially reflected, and two low-finesse optical cavities with physical distances z_1 and z_2 were particularly prominent. Changes in external temperature and pressure resulted in changes to the lengths of these cavities (Δz_1 and Δz_2). Variation in both external temperature and pressure induced changes in z_2, while z_1 only changed in response to temperature due to thermal expansion of the TPP-printed material (data not shown).

The fiber-optic sensor was interrogated with low-coherence interferometry (LCI), as shown schematically in Figure 3. The light source was a superluminescent diode (SLD) with a full-width-at-half-maximum (FWHM) bandwidth of 64 nm centered at 820 nm (BLM-S-280-B-I-10; Superlum, Ireland). Broadband light was provided to the sensor via a 50:50 fiber coupler (TW850R5A2,Thorlabs, NJ, USA). The back-reflected light from the sensor was directed to a spectrometer (Maya 2000Pro, Ocean Optics, FL, USA) via the fiber coupler. To prevent saturation of the spectrometer detector, an in-line

attenuator (VOA-850-APC, Thorlabs) was placed between the source and the coupler. Raw spectra were acquired and processed by a PC running a custom program written with LabVIEW (National Instruments, Newbury, UK), with an overall sampling rate of up to 250 Hz; the actual sampling rate depended on the time taken for raw spectra to be read out and processed by the PC.

In a Fourier transform of the interferogram measured by the spectrometer, distinct peaks corresponding to interference from different surfaces in the sensor were apparent. One prominent peak originated from interference between light reflected from the fiber-optic end-face and the distal surface of the temperature sensitive spacer (z_1). A second peak originated from interference between light from the fiber-optic end-face and the inner surface of the pressure-sensitive diaphragm (z_2). Changes in the complex phase of the Fourier transform at these two peaks were used to monitor deflection of the diaphragm and thermal expansion of the spacer[18,19].

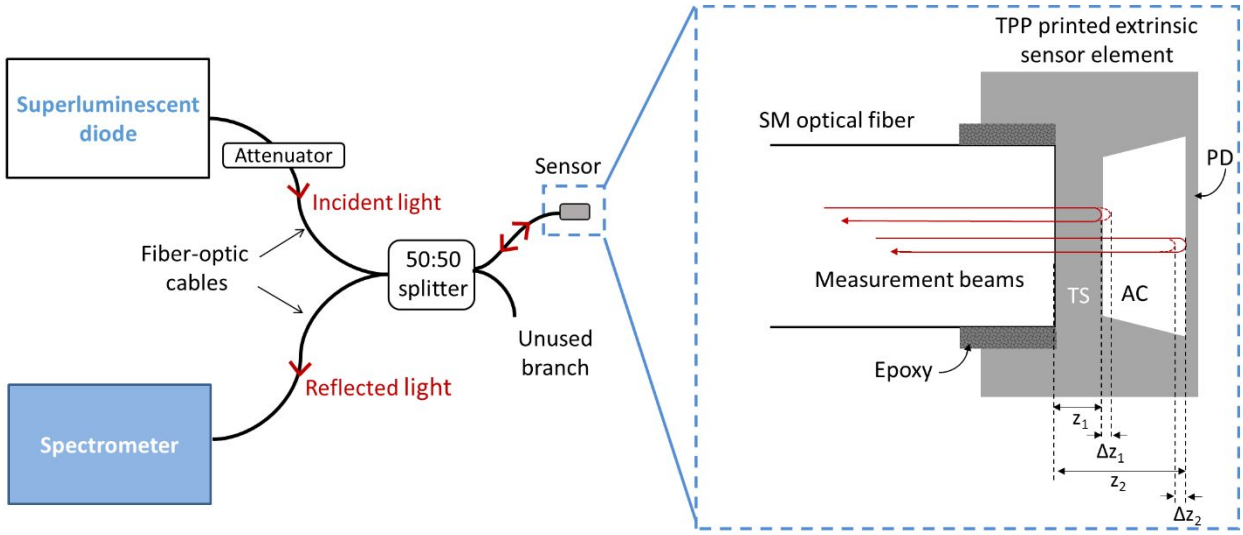

Figure 3. Schematic of the low coherence interferometry (LCI) sensor interrogation system, which included a superluminescent diode as the broadband source, a fiber-optic splitter to deliver light to the sensor, and a spectrometer to measure the interferogram. The sensor comprised the TPP-printed extrinsic sensor element integrated onto a single-mode optical fiber cleaved at normal incidence. Light reflected from multiple surfaces; prominent contributions to the interferogram measured by the spectrometer are indicated ("Measurement beams"; red arrows). These contributions resulted in two distinct peaks in the Fourier-transformed interferogram, which corresponded to low finesse cavities indicated as z_1 (temperature-sensitive) and z_2 (pressure-sensitive and temperature-sensitive). TS: temperature-sensitive spacer; AC: air cavity; PD: pressure-sensitive diaphragm.

2.5 Sensor Characterization

The pressure and temperature responses of the sensor were measured with a pressure-sealed water chamber. Pressure within this chamber was varied with an electro-pneumatic regulator (ITV-0010-3BS, SMC, Japan) and monitored with a custom configured pressure transducer (MMA030USBHB3MC0T8A6CE, Omega Engineering, CT, USA). Pulsed pressure variations with different step sizes and duty cycles were induced within this chamber across the absolute range of 760 mmHg (atmospheric) to 1060 mmHg.

For temperature sensitivity measurements, the chamber was placed in a water bath with a temperature varied from 25 to 47 °C. The reference temperature sensing thermocouple (409-4908, RS Components, UK), which was positioned adjacent to the precision 3D printed fiber-optic sensor. Interferometric phase changes were initially calibrated to values from the corresponding reference sensor with a linear transformation. The pressure within the sealed water chamber was kept constant during temperature sensitivity measurements.

3. RESULTS AND DISCUSSION

3.1 Two-photon polymerization printed extrinsic sensor element

The TPP-printed extrinsic sensor element had an excellent visual correspondence well to its CAD design (Figure 4). Following TPP printing, photoresist development, and detachment from the ITO-coated glass substrate, the extrinsic sensor element was inspected with an optical microscope and a scanning electron microscope (SEM). After photoresist development, no remnant unprocessed excess photoresist material within the cavity space was observed, which indicated that this material was successfully extracted through the conical holes in the spacer. After the integration step, the optical fiber and the extrinsic sensor element were found to be well aligned, by visual inspection. The extrinsic sensor segment assumed a yellow hue after post-illumination with a 405 nm UV LED.

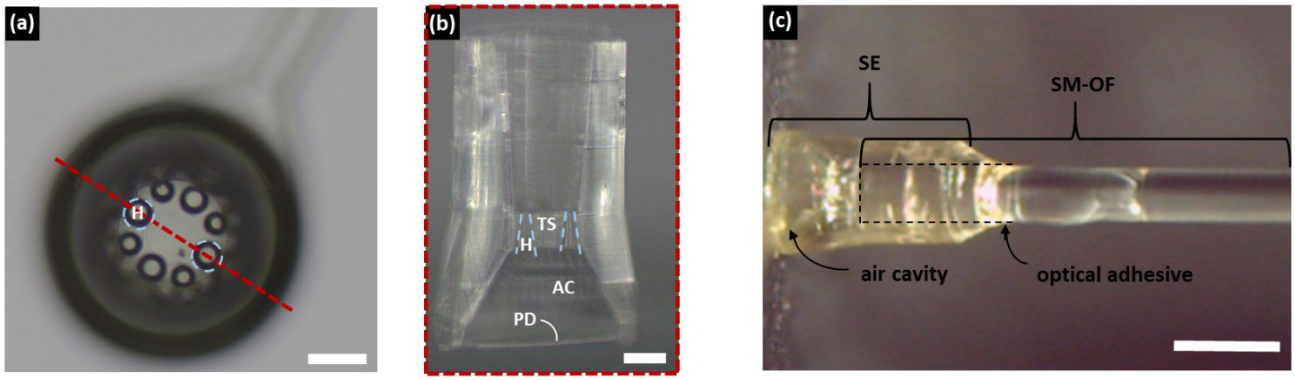

Figure 4. Microscope images of the fiber-optic sensor following two-photon polymerization (TPP) printing, development, and detachment from the substrate. (a) Top view of the sensor, showing the conical hole (H) segments through which unprocessed photoresist material proximal to the pressure-sensitive diaphragm (PD) was removed from within the cavity section (scale bar: 50 µm). (b) Side-view microscope image of a partially-printed extrinsic sensor element with one half [dashed red lines in (a)] intentionally left out for visualization (scale bar: 50 µm).(c) Side-view optical micrograph of the integrated fiber-optic sensor. The optical fiber extended into the region indicated with dashed black lines. SS: sensor segment; SM-OF: single-mode optical fiber (scale bar: 200 µm).

3.2 Pressure and temperature responses

Changes in pressure induced phase shifts in the component of the interferogram corresponding to reflection from the deformable diaphragm (z_2). The unwrapped interferogram phase was initially calibrated to the reference pressure with a linear transformation. Subsequently, its shape well approximated that of the reference pressure signal (Figure 5). In particular, high frequency oscillations following a step change in pressure were observed in both signals. The pressure sensitivity of the sensor was found to be 0.031 rad/mmHg. A noise floor of 12.1 mrad was present in the signal corresponding to reflection peaks from the deformable diaphragm, resulting in a minimum detectable pressure change of 0.38 mmHg. Mechanical hysteresis and signal drift were both apparent; these effects remain to be fully characterized. The sensor was found to be structurally robust to minor impacts against the walls of the water chamber, and to traversal through luer fittings during pressure response tests. The interferogram peaks and the pressure sensitivity were found to be largely consistent across multiple measurement cycles.

Changes in temperature were observed to induce phase shifts in the component of the interferogram corresponding to reflection from the spacer (z_1). This component was found to be insensitive to changes in pressure across the measured range. The temperature sensitivity of the sensor was found to be 0.33 rad/ °C. The observed noise floor in the phase peak of the interferogram corresponding to the distal surface of the spacer was 7.6 mrad, while temperature changes of 0.023 °C were detectable with this sensor.

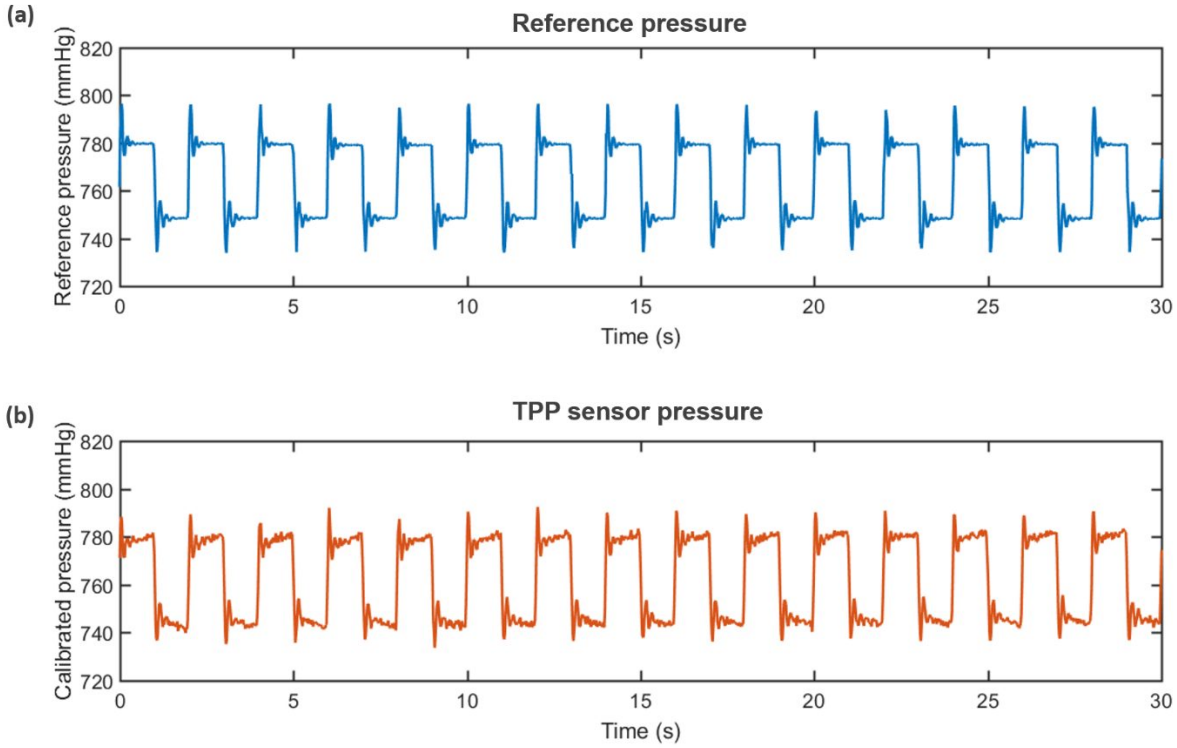

Figure 5. Absolute pressure signals measured concurrently from the pressure-sealed water chamber. (a) Calibrated pressure signal from the TPP-printed fiber-optic sensor, with calibration to the reference pressure signal performed with a linear transformation just prior to acquisition of these data. (b) Reference pressure signal.

4. SUMMARY AND FUTURE WORK

We demonstrated how two-photon polymerization (TPP) printing can be used to fabricate fiber-optic pressure and temperature sensors. To the authors' knowledge, this is the first study to create a 3D-printed fiber-optic extrinsic sensor with a confined air cavity for fiber-optic pressure sensing. A spacer element positioned proximal to the diaphragm allowed for concurrent pressure and temperature measurements with phase-resolved low coherence interferometry. A lateral holding element enabled manipulation of the TPP-printed structure; it was subsequently detached from the extrinsic sensor element, following integration of the single-mode optical fiber.

TPP printing is attractive in this context as it provides sub-micron resolution and 3D micro-fabrication capabilities. It allows for rapid iteration of sensor designs for prototyping, including variation of the thickness and shape of the deformable diaphragm and the incorporation of optical elements proximal to the diaphragm.

There is likely to be scope for significantly improving the mechanical and optical characteristics of the TPP-printed structure, for instance by using a different material and by creating composites with additional materials such as metallic mirrors. For clinical applications involving intravascular pressure sensing, long-term pressure signal drift is a key parameter. The extent that this drift can be minimized with TPP-printed structures remains to be determined.

The design flexibility afforded by TPP printing will likely lead to a new generation of fiber-optic sensors with capabilities that extend beyond pressure and temperature. These sensors could readily be combined with recent innovations in TPP-printing, such as micro-printed optics[14] and tissue manipulators[15], to create versatile tools for minimally invasive surgery.

REFERENCES

[1] Puri, R., Worthley, M. I. and Nicholls, S. J., "Intravascular imaging of vulnerable coronary plaque: current and future concepts," Nat. Rev. Cardiol. **8**(3), 131–139 (2011).

[2] Finlay, M. C., Mosse, C. A., Colchester, R. J., Noimark, S., Zhang, E. Z., Ourselin, S., Beard, P. C., Schilling, R. J., Parkin, I. P., Papakonstantinou, I. and Desjardins, A. E., "Through-needle all-optical ultrasound imaging in vivo: a pre-clinical swine study," Light Sci. Appl. **6**(12), e17103-7 (2017).

[3] Van Soest, G., Regar, E. and Van Der Steen, A. F. W., "Photonics in cardiovascular medicine," Nat. Photonics **9**(10), 626–629 (2015).

[4] Poeggel, S., Tosi, D., Duraibabu, D., Leen, G., McGrath, D. and Lewis, E., "Optical Fibre Pressure Sensors in Medical Applications," Sensors **15**(7), 17115–17148 (2015).

[5] Roriz, P., Frazão, O., Lobo-Ribeiro, A. B., Santos, J. L. and Simões, J. A., "Review of fiber-optic pressure sensors for biomedical and biomechanical applications," J. Biomed. Opt. **18**(5), 50903 (2013).

[6] Yoshino,T., Kurosawa, K., Itoh,K., Oze, T., "Fiber-Optic Fabry-Perot Interferometer and Its Sensor Applications," 1624–1633 (1982).

[7] Saran, A., Abeysinghe, D. C. and Boyd, J. T., "Microelectromechanical system pressure sensor integrated onto optical fiber by anodic bonding," Appl. Opt. **45**(8), 1737 (2006).

[8] Wu, S., Serbin, J. and Gu, M., "Two-photon polymerisation for three-dimensional micro-fabrication," J. Photochem. Photobiol. A Chem. **181**(1), 1–11 (2006).

[9] Maruo, S., Nakamura, O. and Kawata, S., "Three-dimensional microfabrication with two-photon-absorbed photopolymerization," Opt. Lett. **22**(2), 132 (1997).

[10] Göppert-Mayer, M., "Uber Elementarakte mit zwei Quantensprüngen," Ann. Phys. **401**(3), 273–294 (1931).

[11] Wang, H., Xie, Z., Zhang, M., Cui, H., He, J., Feng, S., Wang, X., Sun, W., Ye, J., Han, P. and Zhang, Y., "A miniaturized optical fiber microphone with concentric nanorings grating and microsprings structured diaphragm," Opt. Laser Technol. **78**, 110–115 (2016).

[12] Liberale, C., Cojoc, G., Candeloro, P., Das, G., Gentile, F., Angelis, F. De and Fabrizio, E. Di., "Micro-Optics Fabrication on Top of Optical Fibers Using Two-Photon Lithography," IEEE Photonics Technol. Lett. **22**(7), 474–476 (2010).

[13] Wang, H., Xie, Z., Feng, S. and Zhang, Y., "3D Micro- and Nano Sensing Devices Creation on the Facets of Optical Fibers via Two-photon Lithography," 2016 Prog. Electromagn. Res. Symp. Shanghai, China **3**, 3348 (2016).

[14] Gissibl, T., Thiele, S., Herkommer, A. and Giessen, H., "Sub-micrometre accurate free-form optics by three-dimensional printing on single-mode fibres," Nat. Commun. **7**, 11763 (2016).

[15] Power, M., Thompson, A. J., Anastasova, S. and Yang, G.-Z., "A Monolithic Force-Sensitive 3D Microgripper Fabricated on the Tip of an Optical Fiber Using 2-Photon Polymerization," Small **14**(16), 1703964 (2018).

[16] Dietrich, P.-I., Blaicher, M., Reuter, I., Billah, M., Hoose, T., Hofmann, A., Caer, C., Dangel, R., Offrein, B., Troppenz, U., Moehrle, M., Freude, W. and Koos, C., "In situ 3D nanoprinting of free-form coupling elements for hybrid photonic integration," Nat. Photonics **12**(4), 241–247 (2018).

[17] Li, J., Mu, J., Wang, B., Ding, W., Liu, J., Guo, H., Li, W., Gu, C. and Li, Z. Y., "Direct laser writing of symmetry-broken spiral tapers for polarization-insensitive three-dimensional plasmonic focusing," Laser Photonics Rev. **8**(4), 602–609 (2014).

[18] Choma, M. A., Ellerbee, A. K., Yang, C., Creazzo, T. L. and Izatt, J. A., "Spectral-domain phase microscopy," Opt. Lett. **30**(10), 1162–1164 (2005).

[19] Coote, J., Mosse, S., Noimark, S., Alles, E., Little, C., Loder, C. D., Rakhit, R. D., Finlay, M. C. and Desjardins, A. E., "Fibre-optic pressure and temperature measurements using phase-resolved low-coherence interferometry (Conference Presentation)," SPIE BiOS **10488**, 104880E (2018).